

Animal Model

Biomaterial-Induced Sarcoma

A Novel Model to Study Preneoplastic Change

C. James Kirkpatrick,* Antonio Alves,[†]
Holger Köhler,* Jörg Kriegsmann,*
Fernando Bittinger,* Mike Otto,*
David F. Williams,[‡] and Rosy Eloy[†]

From the Institute of Pathology, Johannes Gutenberg University, Mainz, Germany; Biomatech,[†] Chasse-sur-Rhône, France; and the Institute of Clinical Engineering,[‡] University of Liverpool, Liverpool, United Kingdom*

In the study of carcinogenesis most interest has focused on carcinomas, as they represent the majority of human cancers. The recognition of the adenoma-carcinoma sequence both in humans and in animal experimental models has given the field of basic oncology the opportunity to elucidate individual mechanisms in the multistep development of carcinoma. The relative scarcity of human sarcomas coupled with the lack of adequate animal models has hampered understanding of the molecular genetic steps involved. We present an experimental model in the rat in which a high incidence of malignant mesenchymal tumors arise around a subcutaneously implanted biomaterial. Nine commercially available biomaterials were implanted in a total of 490 rats of the Fischer strain for 2 years. On average, macroscopic tumors were found in 25.8% of implantation sites over a period from 26 to 110 weeks after implantation. The most frequent tumors were malignant fibrous histiocytomas and pleomorphic sarcomas, although fibrosarcomas, leiomyosarcomas, and angiosarcomas readily developed, the latter especially around polyurethane implants. Of particular interest are the results of a detailed histological study of the capsules around the implanted biomaterials without tumors. Here a spectrum of change from focal proliferative lesions through preneoplastic proliferation to incipient sarcoma could be observed. A parallel immunohistochemical study of peri-implant capsules showed that proliferating cell nuclear antigen was of particular help in identifying these atypical proliferative lesions. To our knowledge this is the first description of a sarcoma model in which preneoplastic lesions can

be readily identified and also reproducibly induced. This model provides the molecular biologist with defined stages in the development of mesenchymal malignancy, with which the multistage tumorigenesis hypothesis can be tested, analogous to the well-known adenoma-carcinoma sequence. (Am J Pathol 2000, 156:1455-1467)

In basic oncological research attention has been focused on the multistage hypothesis of cancer development.^{1,2} This has been particularly well demonstrated for the human colorectal adenoma-carcinoma sequence, in which a series of genetic alterations involving mutational activation of oncogenes and inactivation of tumor suppressor genes characterize the development of invasive adenocarcinoma from an adenoma precursor.³⁻⁵ The fact that these tumors are frequent in humans has meant that there has been no scarcity of tissue for the investigation of the various premalignant stages. In addition, animal models for carcinomas, including their preneoplastic stages, are also readily available. Thus, rats fed 4-nitroquinoline 1-oxide develop a spectrum of lesions in the oral mucosa from hyperplasia through dysplasia to squamous cell papilloma and carcinoma.⁶ Mammary adenocarcinoma with the preneoplastic lesions of atypical hyperplasia can be induced in SV40 large T antigen transgenic mice.⁷ Various methods are also available in the rat for the induction of hepatocellular carcinoma via hyperplastic nodules and include a model of folate/methyl deficiency.⁸

By comparison, sarcomas arise much less frequently in humans. This, coupled with the absence of a clearly defined preneoplastic lesion for human sarcomas, has hampered progress in understanding sarcoma tumori-

Supported by a Brite-Euram grant from the European Union, Project 8000 (BRE 2-CT 94.0607) and by the Ministry of Science of the State of Rhineland-Palatinate, Germany.

Accepted for publication December 21, 1999.

Address reprint requests to C.J. Kirkpatrick, Institute of Pathology, Klinikum der Johannes Gutenberg Universitaet, Langenbeckstrasse 1, D-55101 Mainz, Germany. E-mail: kirkpatrick@pathologie.klinik.uni-mainz.de.

genesis. This in turn has prompted the search for suitable animal models of sarcoma. A variety of models exists to create sarcomas, including the subcutaneous implantation of methylcholanthrene-induced sarcoma in Fischer rats⁹ and the induction of visceral angiosarcomas in C57B1/6 mice using dimethyl hydrazine.¹⁰ Newborn Fischer-344 rats have also been used to establish a dimethylnitrosamine-induced model of a malignant mesenchymal nephroma with similarities to the atypical mesoblastic nephroma of infancy.¹¹ Moreover, sarcomas are also known to arise in p53-deficient mice.¹²

Foreign body-induced sarcomas were extensively studied by KG Brand, especially in the 1970s and early 1980s. A variety of mouse strains, such as the CBA/H and CBA/H-T6, were found to be of particular use in eliciting sarcomas following subcutaneous implantation of copolymer films of vinyl chloride/vinyl acetate,¹³ although a broad spectrum of other mouse strains was also tested to determine the role of sex and strain in sarcoma incidence.¹⁴ Using transfer of preneoplastic reactive tissue from one mouse strain to another, it was shown how the size, material composition, and surface properties of the implants modulated tumorigenesis.^{15,16}

In the present paper we describe a rat model of sarcoma using the subcutaneous implantation of eight different biomaterials, including metals and various synthetic polymers. This gives not only a reproducibly high yield of sarcomas but also a spectrum of lesions, beginning with connective tissue hyperplasia through dysplasia to sarcoma, predominantly malignant fibrous histiocytoma, and pleomorphic sarcoma. This relatively simple model should open up the field of sarcoma tumorigenesis to the molecular biologist and allow the multistage hypothesis to be tested, analogous to what has already been performed for carcinoma.

Materials and Methods

Biomaterials

Nine different types of biomaterial (5 polymers, 3 metals, and 1 ceramic) were chosen, all of which are in routine clinical use. These standard medical grade biomaterials were as follows: ultrahigh molecular weight polyethylene (PE), aliphatic polyurethane (PU), polyvinyl chloride (PVC), polymethylmethacrylate (PMMA), silicone (Si), 99% purity titanium (Ti), nickel chromium (NiCr, 78% nickel, 20% chromium), cobalt-chromium alloy (65% cobalt, 27% chromium), and aluminum oxide (Al₂O₃).

Material Characterization

The biomaterial disks were prepared in such a way as to give a smooth surface, which was confirmed by scanning electron microscopy (Hitachi S 800 SEM). The purity of the medical grade biomaterials was confirmed by a combination of conventional physicochemical surface characterization techniques. These were energy-dispersive X-ray analysis, Fourier-transformed infrared spectroscopy, and X-ray photoelectron spectroscopy.

Animals and Implantation Protocol

The Fischer rat, which has a low natural incidence of soft tissue tumor development, was selected as experimental animal. The rats were individually caged and maintained under controlled conditions of temperature, humidity, and lighting. Animals were anesthetized using intramuscular injection of tiletamine-zolazepam (50 mg/kg body weight). Implantation with 3 identical implants per animal was performed in the subcutaneous tissue of the back in young rats 7 to 8 weeks old. Disks of 15 mm diameter and a total surface area of 350 mm² per disk were used. Before implantation, metal samples were sterilized by steam autoclaving, and polymer samples were sterilized by ethylene oxide gas. Controls consisted of sham-operated animals, in which subcutaneous incisions were made without implantation. A maximum follow-up of 24 months included general evaluation of the animal and specific investigation of the implantation site every 2 weeks, when animal weight was recorded.

To increase the likelihood of detecting early stages in the development of tumors around the implants, two principal studies were carried out, ie, at 8 months and 24 months. For the 8-month study each group consisted of 10 rats (5 male, 5 female), each with 3 implantation sites. In addition, from a preliminary study, tissue was also available from a PU and PE group after 3 months of implantation (10 animals per group, 90 animals in total). In the 24-month study, each group consisted of either 30 or 68 rats (50% female), again with 3 implantation sites per animal (490 animals in total).

Histology and Immunohistochemistry

Animals were sacrificed by a lethal intraperitoneal injection of barbiturates once a tumor had reached a mass of approximately 50 g or before this from ethical considerations. This endpoint was determined by estimating from the first sarcomas obtained the tumor size corresponding to a weight of 50 g. A complete autopsy was performed on each animal. All local tumors at the implantation site, as well as any remote tumors, were fixed for histological examination. In addition, all capsules around the implants were preserved for microscopy, irrespective of the presence or absence of a tumor. Tissues were fixed immediately after removal from the sacrificed animals in 10% buffered formalin, embedded in paraffin, and cut into sections 5 μ m thick. Conventional staining was performed with hematoxylin and eosin (HE) and the elastica-van Gieson stain for connective tissue components.

A total of 193 tumors and 312 capsules surrounding the biomaterials was investigated. Buffered formalin-fixed tissues obtained from biomaterial implant sites were sectioned from paraffin blocks in the conventional manner at 5 μ m thickness. Immunohistochemical reactions were performed with a variety of antibodies. Macrophage-detecting antibodies (ED1, diluted 1:50, ED2, diluted 1:50, ED3, diluted 1:200, and KiM2R, diluted 1:100) were supplied by BMA Biomedicals AG (Augst, Switzerland) and

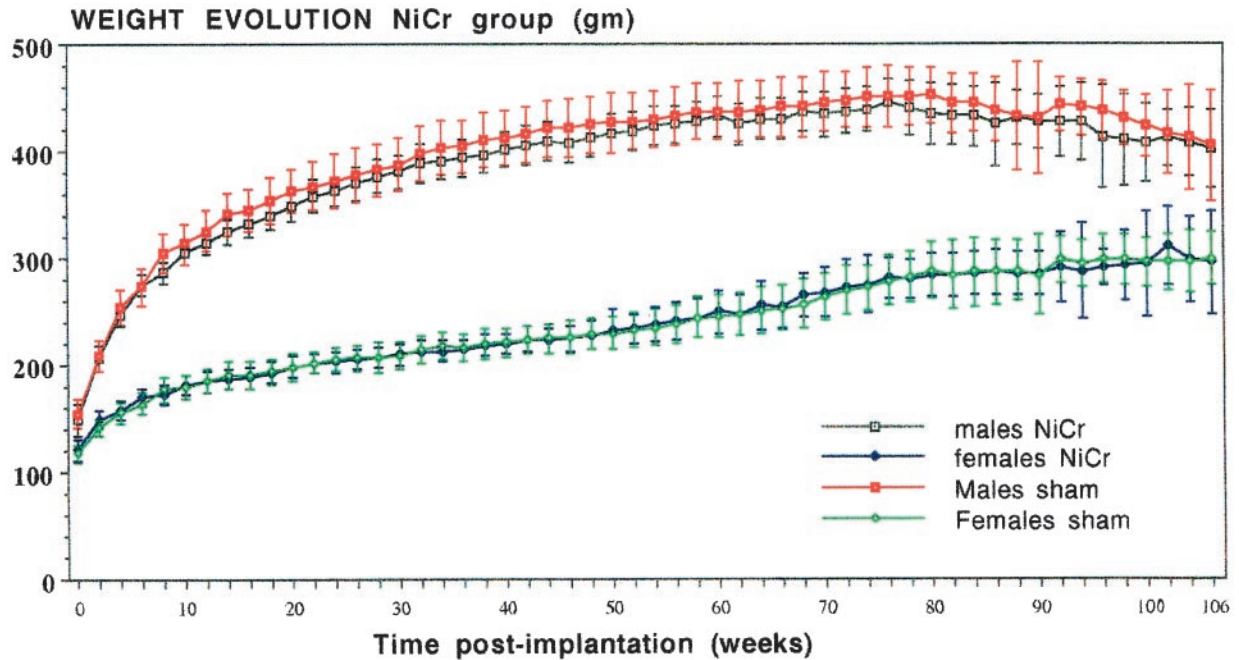


Figure 1. Weight evolution in the group of 68 rats (34 male, 34 female), followed for a maximum of 106 weeks in the NiCr implantation group, compared with the sham-operated control animals. Weight values in grams \pm SD. No statistically significant differences were found.

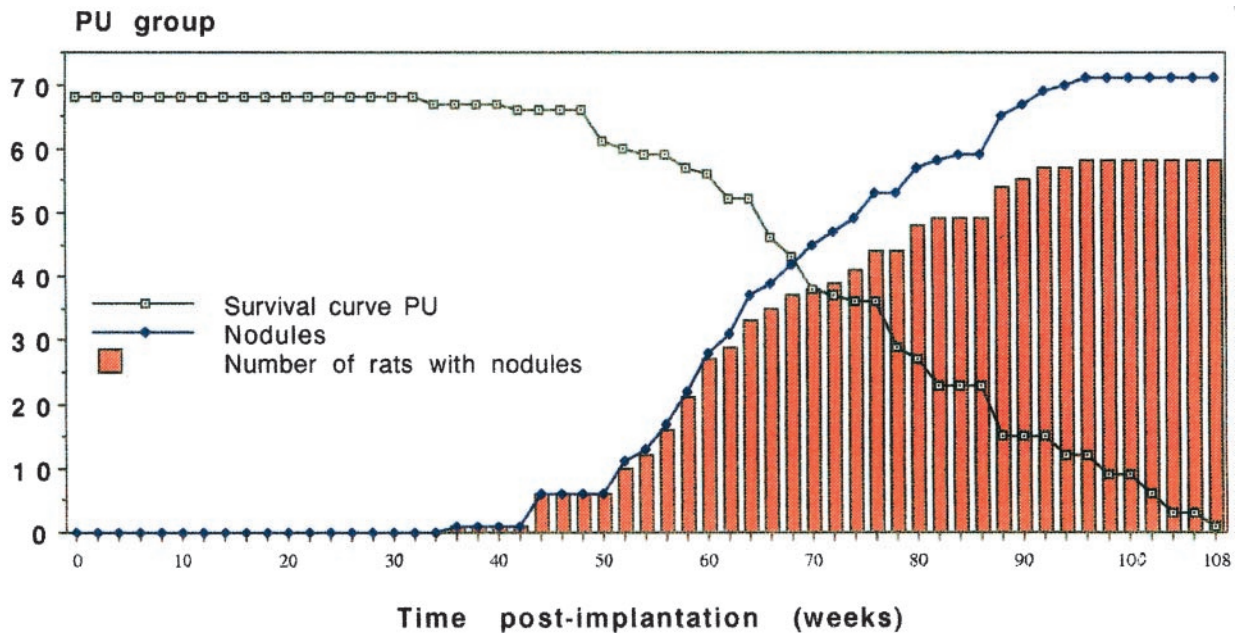


Figure 2. Development of sarcoma in a total of 68 rats (male and female taken together) in the PU group during the 2-year study. The Kaplan-Meier type of survival curve is shown by the open squares. It should be stressed that these curves are based on the endpoint 50 g tumor weight and not on actual survival of tumor-bearing animals. These curves are thus Kaplan-Meier-like. Tumors did not appear until week 36, after which time a steady increase in macroscopically manifest tumors arose (\blacklozenge). The number of rats bearing tumors is shown by the histograms. The latter values are below those for the number of tumors, as some rats carried more than one tumor.

used after trypsin pretreatment. Visualization was achieved using either avidin-biotin complex (ABC) or alkaline phosphatase-anti-alkaline phosphatase protocols. T cells were stained with the antibodies MAS 010 and MAS 041 (each diluted 1:150), supplied by Sera Feinbiochemica GmbH (Heidelberg, Germany) and visualized using the ABC protocol. B lymphocytes were de-

tected with the antibody MAS 258 (KIB 1R, Sera), diluted 1:200, using the ABC method after trypsinization. Finally, the proliferating cell nuclear antigen (PCNA) antibody (DAKO Diagnostika GmbH, Hamburg, Germany) was used with an ABC protocol after microwave treatment of the sections. Controls consisted of the use of an irrelevant antibody or omission of the primary (specific) antibody.

Table 1. Development and Frequency of Sarcomas in Biomaterial Groups

Implant group	Earliest sarcoma (weeks)	% of implantation sites with sarcoma at 2 years
Polyethylene	26	35
Polyurethane	36	35
Polyvinylchloride	40	24
Polymethylmethacrylate	50	20
Silicone	52	31
Titanium	48	12
Nickel-chromium	46	33
Aluminum oxide	42	23

Statistical Analysis

The weight change between a particular implant group and the sham-operated controls was tested for statistical significance using the one-way analysis of variance parametric test, followed by the Scheffé test *a posteriori*. Statistical significance was placed at the 5% confidence level.

Results

Tumor Incidence

At 2 years (week 104), 340 tumors had developed from a total of 1266 implantation sites, with 48 animals bearing more than one tumor. The control (sham-operated) animals had no tumor development at any incision site. Generally, once a tumor became visible, rapid growth was observed over a period of 3 to 4 weeks.

Figure 1 presents a typical curve of weight evolution, exemplified by the rats in the NiCr implant group, compared with their sham-operated controls. No statistically significant differences could be detected. This applied also for most implant groups.

The induction of sarcomas took place at varying rates in the different implant groups. Table 1 presents a summary of the most important data, namely the time of first appearance of a sarcoma and the percentage of implantation sites in animals (irrespective of gender) bearing macroscopic soft tissue tumors at the end of the 2-year observation period. Figure 2 illustrates a typical cumulative display of sarcoma development with time, as well as a survival curve for the PU group.

The high incidence of sarcoma induction is well illustrated by the balance at the end of the 2-year observation period. Thus, out of 68 animals in each group, only 1 was tumor-free in the PU group. The values for PE, NiCr, and Ti are 4, 5, and 21 respectively.

Histological Tumor Type

All tumors at biomaterial implantation sites were of mesenchymal origin. However, no correlation could be established between biomaterial groups and a specific histological type of tumor, although the PU group did exhibit a

Table 2. Cumulative Frequency of Different Histological Tumor Types

MFH	65
Pleomorphic sarcoma	34
Sarcoma with mixed differentiation	22
Sarcoma NOS	21
Fibrosarcoma	23
Leiomyosarcoma	6
Malignant hemangiopericytoma	6
Hemangiosarcoma	2
Miscellaneous	14

tendency to form hemangiosarcomas. The most frequently encountered tumor was the malignant fibrous histiocytoma (MFH), followed by pleomorphic sarcomas. Many cases exhibited mixed differentiation patterns. Table 2 gives the absolute incidence of the various histological types in a total population of 193 tumors from all groups. These sarcomas were seen to be locally invasive, with infiltration of fatty connective tissue and, in many cases, of skeletal muscle. Multiple foci of necrosis were frequently observed.

The morphological characteristics of these tumors are illustrated in Figure 3, which demonstrates not only the most frequently encountered soft tissue tumors, such as MFH (Figure 3A), pleomorphic sarcoma (Figure 3B), and fibrosarcoma (Figure 3C), but also some of the rarer tumors, such as leiomyosarcoma (Figure 3D) and osteosarcoma (Figure 3E). In addition, based on a distinctive cytological appearance of the tumor cells, we recognized individual cases that we termed epithelioid sarcoma (Figure 3F) and round cell sarcoma (Figure 3G). Ranked third in incidence were the sarcomas that could not be placed in one category because substantial parts of the tumor mass exhibited more than one differentiation pathway. These tumors were classified as sarcomas with mixed differentiation and often showed the combination of MFH with a vascular element, usually hemangiosarcoma or hemangiopericytoma (Figure 4A). The pure hemangiosarcomas often gave the appearance on low-power microscopy of a spongy tissue (Figure 4B). High-power examination revealed the clearly atypical nuclei of the cells lining these sponge-like spaces and various degrees of vessel branching (Figure 4C). One vascular tumor that developed around a NiCr implant showed some features reminiscent of papillary hemangioendothelioma (Figure 4D). Occasionally, hemangiosarcomas were highly cellular and, in one case around a titanium implant, demonstrated a high level of apoptosis (Figure 4, E and F). Sarcomas that presented no identifiable differentiation pathways were classified as sarcoma not otherwise specified (NOS). This group accounted for the fourth highest incidence among all tumors (Table 2 and Figure 3H).

Capsule Histopathology

The time after implantation at which capsule tissue became available was generally determined by the decision to sacrifice, based on the presence of a macroscopically manifest tumor. This meant that a broad spectrum of

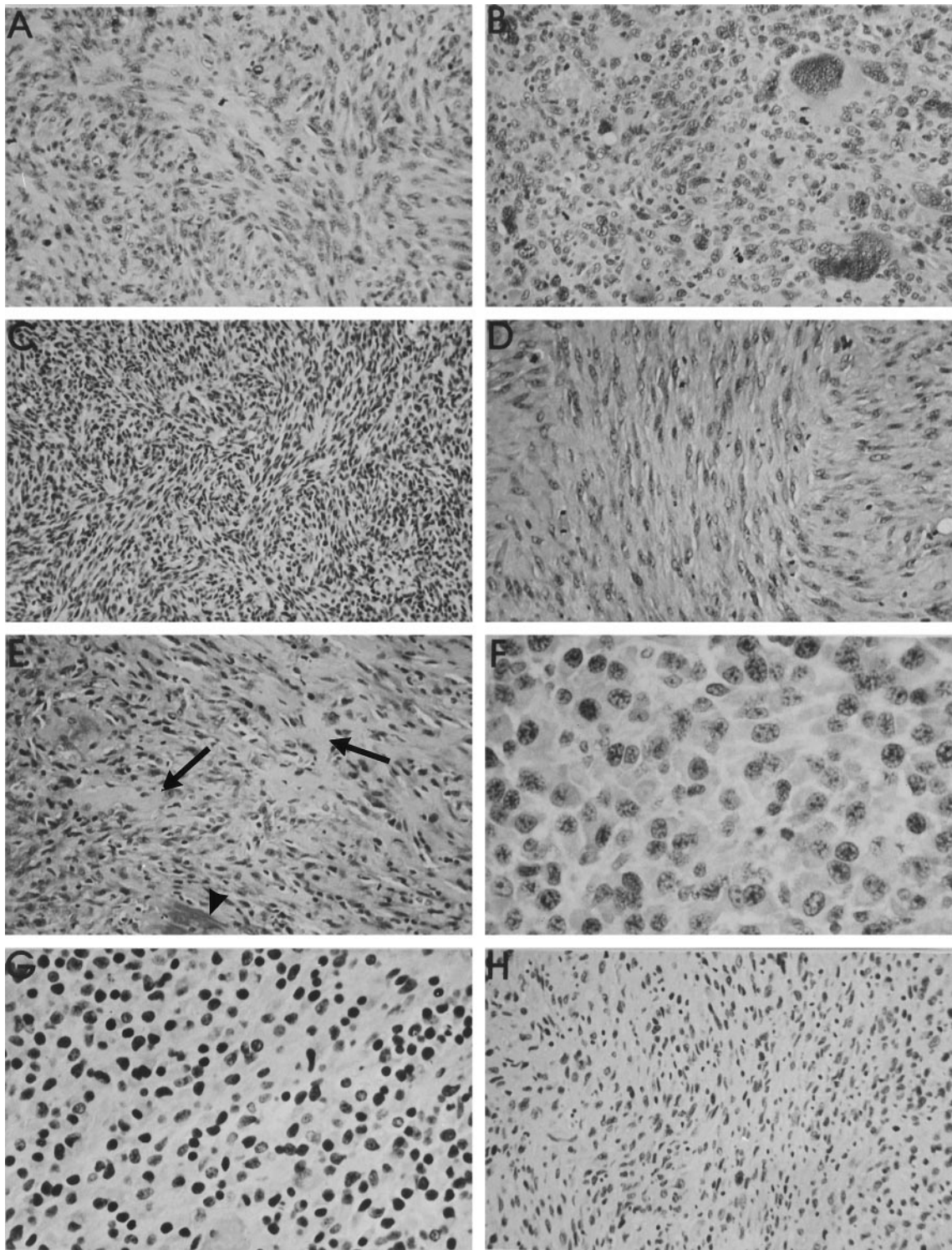


Figure 3. Representative histological types of soft tissue tumors arising around various subcutaneous implanted biomaterials (all HE stain). **A:** MFH around a PE implant at 101 weeks, showing a mild storiform pattern and numerous mitotic figures. **B:** Pleomorphic sarcoma around a PU implant with many large cells with bizarre hyperchromatic nuclei. **C:** Fibrosarcoma induced by an Al_2O_3 implant at 103 weeks. Interweaving bundles of small spindle cells are demonstrated. **D:** High mitotic rate in a leiomyosarcoma around a Ti implant at 107 weeks with typical blunt-ended vesicular nuclei. **E:** Foci of osteoid matrix (arrows) in an osteosarcoma induced by a PMMA implant after 84 weeks. Foci of calcified matrix were also seen (arrowhead). **F:** PU-induced epithelioid sarcoma with markedly polygonal tumor cells. **G:** Small hyperchromatic nuclei in a round cell sarcoma induced by a PU implant after 80 weeks. **H:** Anisomorphic nuclei in a sarcoma around a Si implant after 90 weeks. No specific morphological pattern identifiable. Hence the classification sarcoma NOS. Objective magnifications, $\times 40$ (F and G) and $\times 20$ (all others).

times of exposure to the biomaterials became available for histopathological evaluation. In general, a thin fibrous connective tissue capsule of approximately 300 μm

formed around the entire circumference of the subcutaneous implant (Figure 5A). Histopathological examination revealed a variety of morphological entities, which were

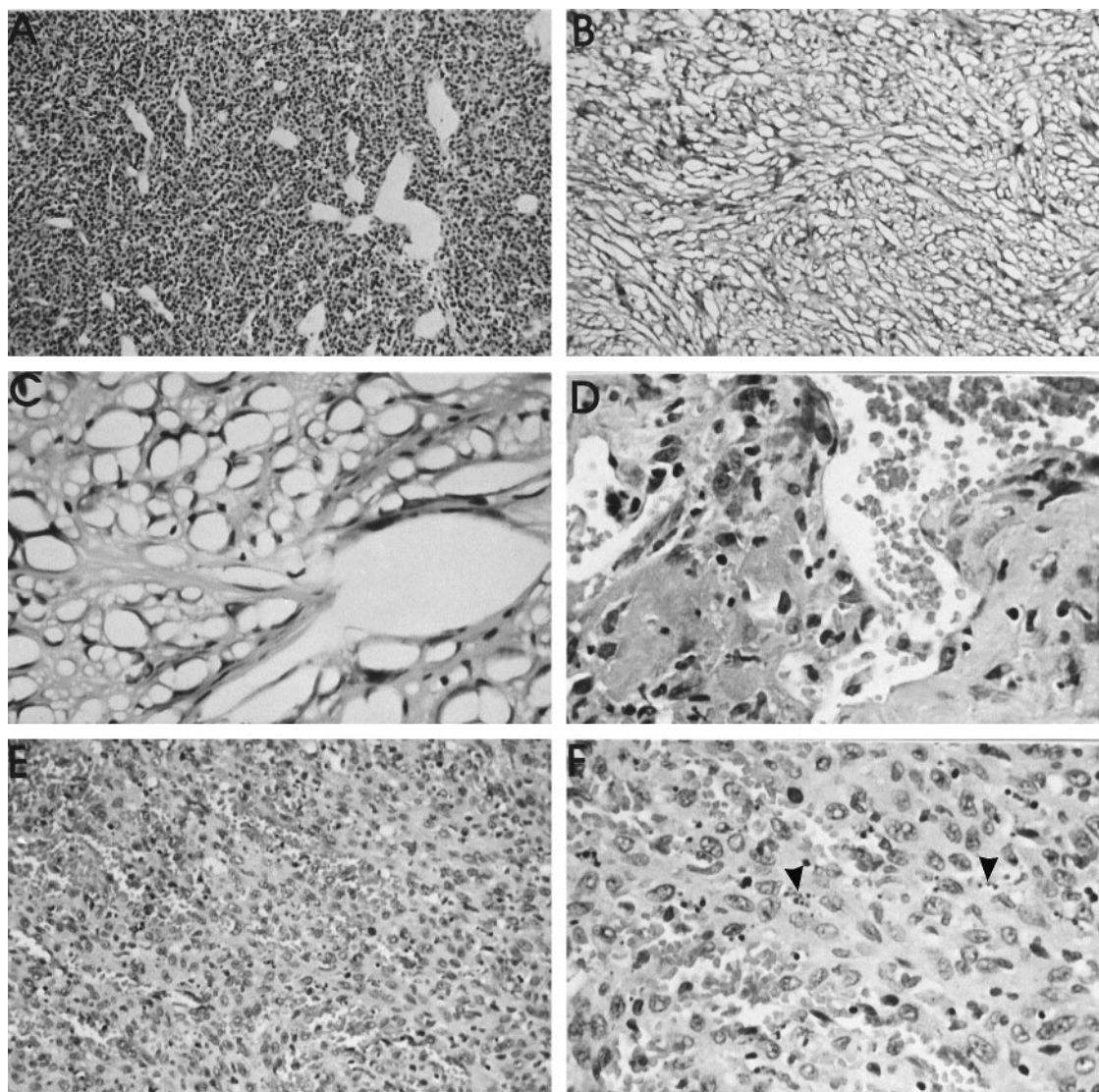


Figure 4. Histological appearance (HE stain) of sarcomas of vascular origin. **A:** Malignant hemangiopericytoma around an Al_2O_3 implant after 46 weeks. Vascular channels of various calibers and shapes are surrounded by relatively small, polygonal cells. Objective magnification, $\times 10$. **B:** Characteristic low-power (objective magnification, $\times 10$) of a PU-induced hemangiosarcoma, giving a spongy appearance. **C:** Higher power view (objective magnification, $\times 40$) to demonstrate vessel branching. The numerous tumor vascular spaces are formed by cells with markedly hyperchromatic nuclei. **D:** Malignant papillary hemangioendothelioma around a NiCr implant at 107 weeks. High-power view (objective magnification, $\times 40$), illustrating two papillary elements, consisting of pleomorphic cells and numerous vascular channels. **E:** Highly cellular form of an hemangiosarcoma, induced at 90 weeks by a Ti implant. The high degree of vascularity is apparent. Objective magnification, $\times 20$. **F:** Higher power view of the cellular hemangiosarcoma to demonstrate the marked level of apoptosis (arrowheads). Objective magnification, $\times 40$.

clearly distinguishable from each other. As was the case for the histological type of tumor developing around a biomaterial, no association could be established between the biomaterial type and the capsule reaction. In addition to paucicellular fibrous tissue capsules, focal or extensive proliferative lesions were observed (Figure 5B). These proliferative lesions consisted of groups of polygonal and/or spindle cells, usually in the inner portion of the capsule, adjacent to the biomaterial (Figure 5C). A further morphological variation took the form of a proliferative lesion, but with the additional feature that discrete cellular atypia were present, which could not be definitively categorized as preneoplastic. These lesions were therefore termed proliferative lesions, possibly preneo-

plastic (Figure 5D). In many cases, however, foci of proliferation were observed with marked cellular atypia, such as cellular and nuclear pleomorphism, coupled with hyperchromasia and well-defined nucleoli (Figure 5E). These capsules were designated as preneoplastic lesions. A few capsules revealed a further stage in the development of a sarcoma and showed usually a larger area of markedly atypical cells with an organoid pattern. These lesions could be clearly identified as malignant, but as they were macroscopically unable to be detected, we termed them incipient sarcoma (Figure 5F).

Certain cases presented a combination of lesions, such as a manifest sarcoma (also macroscopically apparent) and a preneoplastic lesion. Figure 5G shows the

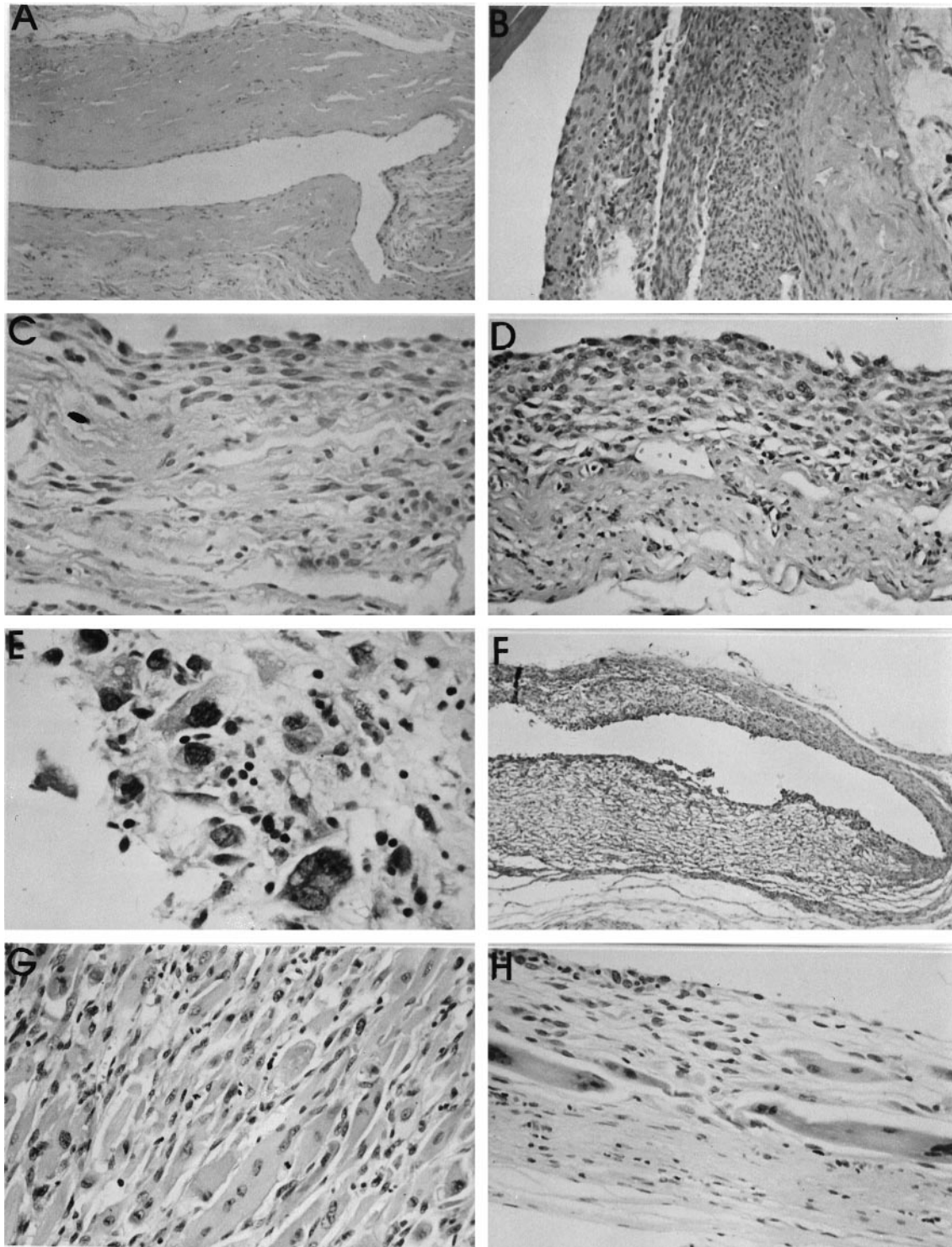


Figure 5. **A:** paucicellular fibrous tissue capsule from around a NiCr implant at 93 weeks. **B:** Proliferative lesion around a Ti implant after 106 weeks. No cellular atypia could be distinguished. **C:** Inner surface of a peri-implant capsule (Si implant at 107 weeks), showing a mixed population of polygonal and spindle-shaped cells, but without atypia. **D:** Capsule tissue from around a PMMA implant. The capsule is both vascular and cellular, with some pleomorphic, vesicular nuclei. The lesion was classified as a proliferative lesion, possibly preneoplastic. Objective magnification, $\times 20$. **E:** High-power view (objective magnification, $\times 40$) of a thin capsule around a Si implant. The innermost layer, immediately adjacent to the implant surface shows hyperchromatic nuclei in markedly pleomorphic cells, some of which are multinucleated. The capsule was designated as a preneoplastic lesion. **F:** Low-power view (objective magnification, $\times 5$) of the entire capsule thickness (ie, both superficial and deep layers) around a PU implant. Both layers are highly cellular, but a hemangiosarcoma has developed in the superficial layer of the capsule (lower half of figure). This was not seen macroscopically. **G:** Histological appearance of a rhabdomyosarcoma, which developed in the deep capsule layer around a PU implant after 101 weeks. The cells contain abundant eosinophilic cytoplasm and pleomorphism and focal vesicularity of nuclei. Objective magnification, $\times 20$. **H:** Superficial capsule layer of the same case as in **G**, showing a thin cellular layer of maximal 12 cell layers. However, large cells with abundant cytoplasm and nuclear pleomorphism are evident. This is a preneoplastic lesion with a rhabdomyoblastic phenotype. Objective magnification, $\times 20$. All stained with HE.

Table 3. Capsule Histology after Short-Term Implantation (3 or 8 months)

Lesion type	PE	PU	PVC	PMMA	Si	Ti
Fibrous capsule	6 (33)	0 (0)	10 (56)	10 (50)	4 (20)	2 (10)
Proliferative lesion						
focal	8 (44)	10 (56)	8 (44)	10 (50)	6 (30)	14 (70)
extensive	0 (0)	2 (11)	0 (0)	0 (0)	0 (0)	0 (0)
Proliferative lesion possibly preneoplastic	4 (22)	6 (33)	0 (0)	0 (0)	10 (50)	4 (20)
Preneoplastic lesion	0 (0)	0 (0)	0 (0)	0 (0)	0 (0)	0 (0)
Number of capsules	18	18	18	20	20	20

Absolute values are presented along with percentage of cases with specific lesions (in parentheses).

histology of a manifest tumor which developed on the deeper surface of a PU implant. This tumor was classified as a rhabdomyosarcoma and clearly demonstrated large tumor cells with abundant eosinophilic cytoplasm. The superficial (ie, overlying the implant) capsule layer was macroscopically a thin fibrous capsule. However, histologically this layer contained some foci with abnormal connective tissue cells, showing a rhabdomyoblastic phenotype (Figure 5H). These cells were clearly atypical, were topographically completely isolated from the rhabdomyosarcoma on the deeper capsule layer, and were therefore regarded as a preneoplastic lesion.

Concerning the incidence of the various capsule lesions, Table 3 shows data from the investigation of the short-term implant capsules, that is, after 8 months (after 3 and 8 months in the case of PU, and after 3 months in the case of PE). Extensive proliferative lesions characterized the PU group, which along with the Si group gave the highest incidence of proliferative lesions with possible preneoplastic change (33 and 50%, respectively). However, in the short-term study no unequivocal diagnosis of a preneoplastic lesion could be made. An important observation was that the Ti group revealed a high incidence (70%) of focal proliferative lesions but, in the long term, the lowest incidence of sarcoma development.

From about month 10 as sarcomas developed, an increasing number of capsules became available for histopathological examination in which no macroscopic tumor had been observed. The majority of animals with sarcoma had developed it at one implantation site, so that at time of sacrifice two additional capsules became available which were macroscopically normal. The most important data from this study are summarized in Table 4, which shows the percentage of incidence of capsule lesions in the various implantation groups studied from

month 8 onward. It must be stressed that the sarcoma cases listed in this table represent tumors that were macroscopically not evident. The incidence of these small sarcomas and incipient sarcomas was particularly high in the PE and NiCr groups (34 and 24%, respectively). Concerning the interesting group of clearly diagnosable preneoplastic lesions, the highest incidence was observed in the PMMA and Si groups, with values of 39 and 25%, respectively.

In the immunohistochemical study, which was intended to identify relevant cell populations in the vicinity of the biomaterials, some surprising results were obtained. This study was hampered by the restricted availability of commercial antibodies to rat antigens. In general, specimens from various sarcomas and capsule tissue with the different lesions (presented in Tables 3 and 4) showed focal accumulations of macrophages and B lymphocytes without giving any pattern which could be defined as typically associated with a specific lesion. Thus, a specific leukocyte reaction could not be documented, either in the stable (fibrous) capsules or in the capsules with proliferative or preneoplastic lesions. Of greater importance, the immunohistochemical staining pattern of the preneoplastic lesions gave data that were inconsistent with the available information on specificity of reaction of the antibodies. This became apparent in a detailed immunohistochemical study carried out on 7 randomly selected cases of diagnosed preneoplastic lesion (capsules from 2 cases of PMMA, 2 cases of Ti, and 1 case each of PVC, PE, and NiCr). In all cases the atypical cell population, whether of spindle cell or polygonal cell morphology, gave a strongly positive reaction with PCNA in 90 to 95% of cells (Figure 6, A and B). This also applied to such lesions, as illustrated in Figure 6C, in which the cellular focus was only 5 to 6 cell layers thick.

Table 4. Capsule Histology after Long-Term Implantation (8 months onward)

Lesion type	PE	PU	PVC	PMMA	Si	Ti	NiCr	Al ₂ O ₃
Fibrous capsule	8 (25)	7 (33)	8 (44)	6 (33)	3 (19)	21 (48)	10 (30)	8 (50)
Proliferative lesion	4 (13)	3 (14)	2 (11)	0 (0)	2 (13)	4 (9)	5 (15)	3 (19)
Proliferative lesion, possibly preneoplastic	4 (13)	5 (24)	2 (11)	3 (17)	4 (25)	4 (9)	3 (9)	1 (6)
Preneoplastic lesion	4 (13)	3 (14)	4 (22)	7 (39)	4 (25)	8 (18)	2 (6)	2 (13)
Sarcoma	11 (34)	3 (14)	1 (6)	2 (11)	1 (6)	4 (9)	8 (24)	1 (6)
Number of capsules	32	21	18	18	16	44	33	16

Absolute values are presented along with percentage of cases with specific lesions (in parentheses).

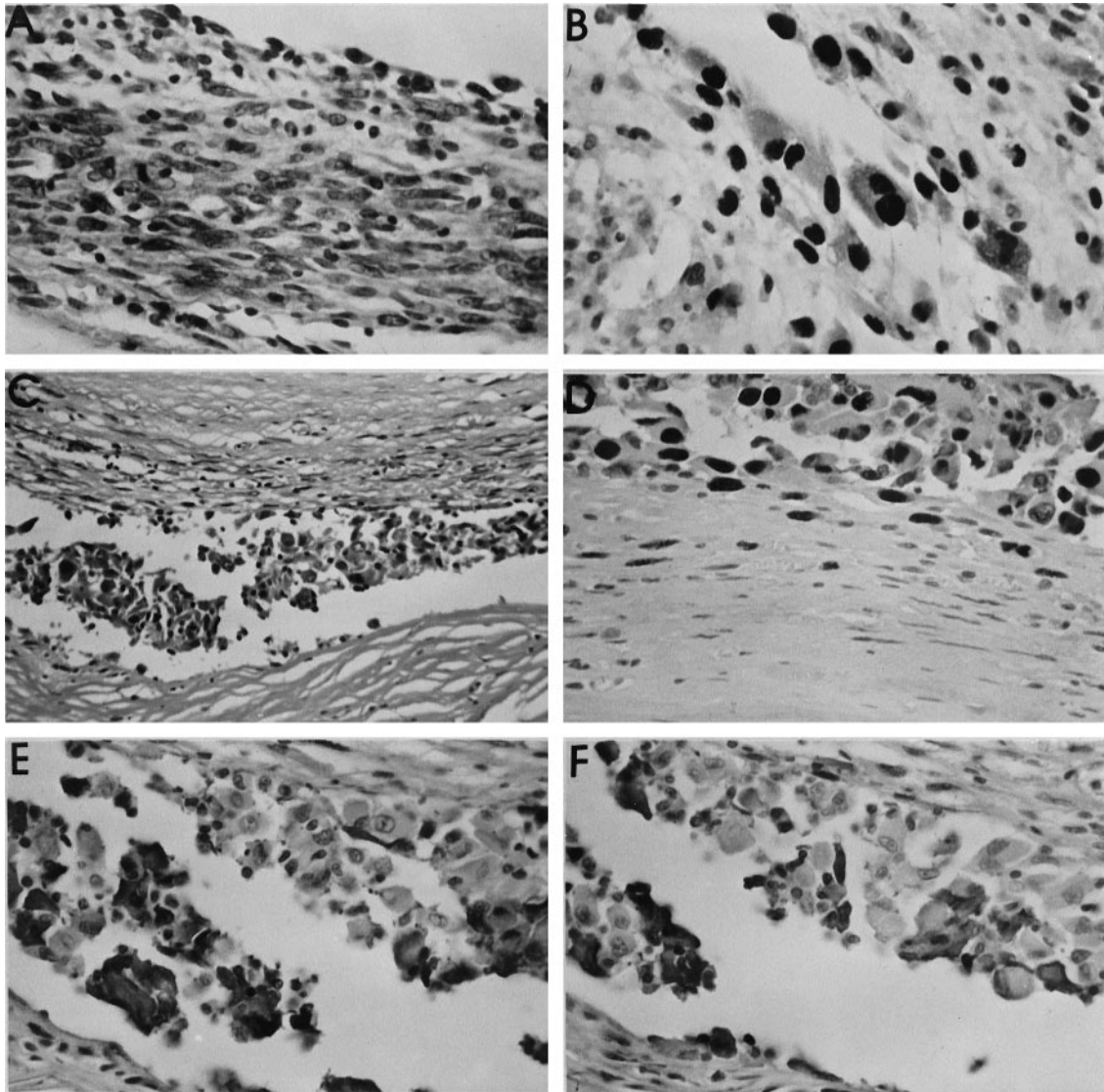


Figure 6. Immunohistochemical study of preneoplastic lesions. **A:** Very cellular, preneoplastic lesion in a capsule around a Ti implant. Marked cellular atypia are seen (HE stain). **B:** PCNA immunohistochemistry of the same lesion as in **A**. Note the intense nuclear staining in the majority of the atypical cells. **C:** Premeoplastic lesion in the capsule surrounding a PMMA implant. Despite the relatively thin cellular layer, many cells demonstrate clear atypia (HE stain). **D:** Marked PCNA staining of the atypical cells in the same case as in **C**. These cells were immediately adjacent to the implant (upper portion of figure). A gradient of PCNA positivity was observed from the implant toward the peripheral part of the capsule, so that here (lower portion of figure) spindle-shaped fibroblastic cells without atypia showed only faint or no positivity. **E:** Same case as in **C**, showing the immunohistochemical reaction with the KiB1R antibody directed against B lymphocytes. A subpopulation of the atypical cells is stained positively. **F:** Same case as in **E**, demonstrating a positive subpopulation of atypical cells in the preneoplastic lesion staining for the KiM2R antibody, directed against activated macrophages. Original magnifications, $\times 20$ (**C**) and $\times 40$ (all others).

The atypical nuclei stained intensely with PCNA (Figure 6D). Figure 6D also demonstrates an important phenomenon, namely the definite gradient of positivity from the dense staining of the atypical nuclei adjacent to the site of the biomaterial to complete negativity of quiescent fibroblasts in the deep part of the capsule. The problematic data derive from the immunohistochemical examination using the inflammatory cell markers. Figure 6E shows the reaction of a PMMA capsule to the B lymphocyte marker, KiB1R. This antibody recognizes an epitope on a subpopulation of the atypical cells. A similar biphasic staining pattern, ie, some cells positive, some negative, was obtained for the KiM2R antibody, which should identify activated macrophages (Figure 6F).

In summary, only one immunohistochemical reaction yielded data that could be interpreted readily. PCNA expression was an excellent method to localize both the preneoplastic lesions and those designated as proliferative and possibly preneoplastic.

As a result of ethical considerations, animals were sacrificed once tumors had become manifest. This meant that no further possibility existed in the experimental model to study metastatic behavior of these tumors over a defined period of time. Nevertheless, in 8 animals, 4 of which were in the polyurethane group, distant metastasis of the sarcomas did occur. Figure 7 illustrates this for a sarcoma around a PU implant. At the time of sacrifice (87 weeks) multiple pulmonary

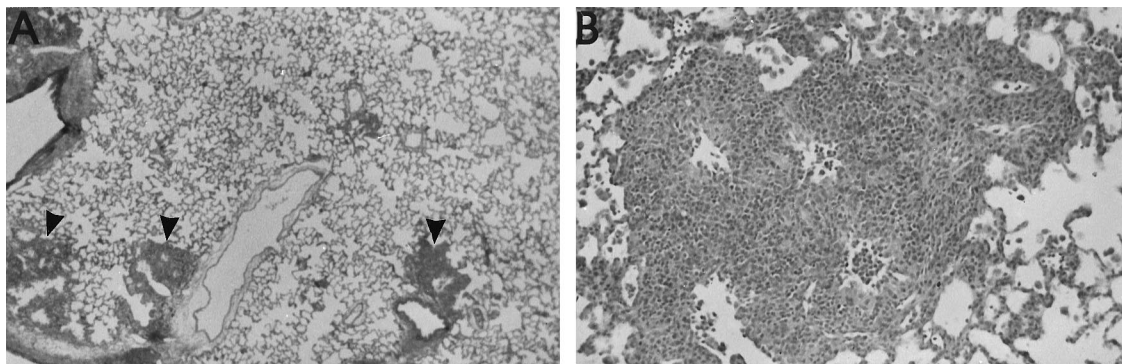


Figure 7. A: Lung tissue from a rat at 87 weeks after implantation with PU. Multiple tumor nodules are seen (arrowheads). Objective magnification, $\times 2.5$. **B:** Higher power (objective magnification, $\times 10$) of a pulmonary tumor nodule, showing sarcoma metastasis. The phenotype was that of a round cell sarcoma. All stained with HE.

metastases were observed, the phenotype being that of a round cell sarcoma.

Discussion

The ability of biomaterials or their breakdown products to induce cancer is of increasing importance in the constantly expanding medical device field. Although certain applications, such as silicone breast implantation, show no documented human cases of sarcoma development,¹⁷ there is increasing concern that in the long term arthroplasty implants may be associated with cancer. A more recent study on hip arthroplasty indicates that chromosomal aberrations can frequently be found in the adjacent bone marrow.¹⁸ In the literature biomaterial-induced sarcomas have been described in various animal models. Thus, using 11-week-old male Wistar rats, Nakamura et al were able to induce predominantly fibrosarcoma and MFH by subcutaneous implantation of slowly degradable poly-L-lactide plates.¹⁹ Medical grade polyethylene was used as control and also induced sarcomas. Furthermore, in the field of orthopedic implants it has been shown that intra-articular injection of nickel subsulfide in Fischer-344 rats induces poorly differentiated or pleomorphic sarcomas.²⁰

The F-344 rat model has also been used to study the early cellular response to subcutaneous implants at 1 week and 2 months postimplantation.²¹ Silicone elastomer and impermeable cellulose acetate filters (pore size $<0.02 \mu\text{m}$) were taken as two positive groups, known to induce sarcoma after about 11 months, and compared with porous cellulose acetate filters (pore size $>0.65 \mu\text{m}$), which are noncarcinogenic. This latter group was found to have less cell proliferation, apoptosis, and fibrosis, but more extensive inflammation than the two tumorigenic implants, which could not be distinguished from each other on the basis of the parameters chosen.

A study of the literature makes it abundantly clear that there are relatively few models available which present early stages of sarcoma development. This is in marked contrast to the situation for carcinomas, in which both human and animal tissues are available for study and

which include clearly defined premalignant stages.³⁻⁸ Expression of the human immunodeficiency virus *tat* gene in transgenic mice has been shown to induce leiomyosarcomas and early stages of Kaposi's sarcoma in the skin.²² The transgenic mouse model has also been used to express the bovine papillomavirus type 1 genome, leading to development of dermal fibromatosis and fibrosarcomas.²³ Chromosomal studies revealed that only in the latter group could aberrations be detected, which in this sarcoma involved chromosome 8 (trisomy or duplication) and chromosome 14 (monosomy or translocation). As early as 1983, Rachko and Brand used subcutaneous implantation of a copolymer of vinyl chloride acetate in two mouse strains to induce sarcomas.²⁴ They described 6 cases of preneoplasia derived from the peri-implant tissue taken at 4, 6, 9, and 16 months postimplantation. Using their mouse model, Brand and colleagues established a hypothetical model to describe the stages of foreign body tumorigenesis.²⁵ Their proposed sequence involved an initial phase of proliferation with the acute foreign body inflammatory reaction, followed by capsule fibrosis, quiescence of phagocytic activity, and, finally, direct contact between material and clonal preneoplastic cells. Further investigations by this group documented [³H]-thymidine labeling of predominantly macrophages attached to the copolymer film used as implant²⁶ as well as a temporary repression of fibronectin synthesis in the early stages of preneoplasia.²⁷ In addition, aromatic amines have been used to induce splenic sarcomas in F-344 rats.²⁸ In that model splenic fibrosis and capsule hyperplasia were described as preneoplastic lesions.

It should be stressed here that the sarcoma induction mechanism involves direct contact with the biomaterials. Thus, this model is limited to signals that are elicited locally. The role of systemic factors in the induction process remains completely unknown, as does the differentiation between local chemical and physical characteristics as the predominant pathogenetic factor. Nevertheless, it may be speculated that the chemical component might be minimal, as the biomaterials span a vast spectrum of chemical structure (polymers, metals,

ceramic), so that to implicate chemical sarcomagenesis as the prime factor would suggest that a number of compounds of entirely different chemical composition can, under the implantation conditions described here, induce tumors with relatively high incidence. Theoretically, it is possible that residual monomers from the polymer synthesis and/or compounds used in the plasticizing process or other leachables could play a role, although the fact that the materials used were of medical grade and thus pretested for negative effects of leachables makes this hypothesis improbable. In the case of the metals the chemical carcinogenesis mechanism is much more feasible, as it has been shown in numerous studies that metallic elements used in surgical alloys, including cobalt, can act as chemical carcinogens.²⁹ The complexity of this topic is indicated by the studies of Meachim and colleagues,³⁰ who were unable to induce sarcoma in rats or guinea pigs with intramuscular implantation of particulate debris of cobalt-chromium-molybdenum (CoCrMo), and Lewis et al.,³¹ who failed to induce sarcomas by intra-articular injection of Fischer-344 rats with CoCrMo or titanium-aluminum-vanadium powders. With respect to possible chemical induction from the aluminum oxide ceramic material, very interesting data are to be found in the veterinary pathology literature, where fibrosarcomas are especially known to arise in cats at vaccination sites after feline leukemia virus and rabies vaccination.^{32,33} Using electron probe microanalysis, Hendrick and colleagues succeeded in demonstrating that aluminum oxide from the vaccine adjuvant was present in tumor-associated macrophages and suggested that this could be involved in the development of neoplasia.³⁴ Support for a primarily physical pathogenetic factor comes from the fact that the biomaterial implants, although of varied chemistry, were prepared as disks in such a way that the surface roughness did not differ markedly. It has been known for a long time (the so-called Oppenheimer effect³⁵) that solid materials that are not degradable and have a relatively smooth continuous surface are tumorigenic when implanted in rodents, as in the present study.

The lack of correlation between biomaterial composition and the histological type of sarcoma induced is also worthy of discussion. Although not statistically significant, there was an observed trend that polyurethane implants were often associated with vascular tumors. Nevertheless, the total tumor bank from the study covered a wide spectrum of histological types, including angiosarcoma, leiomyosarcoma, rhabdomyosarcoma, fibrosarcoma, pleomorphic sarcoma, and MFH. This fact supports the induction of different differentiation pathways in a mesenchymal stem cell of considerable pluripotency. The lack of effective localizing antibodies for rat epitopes will, unfortunately, continue to hamper the identification of this cell type. At this point it is also important to address the vexed question of sarcoma terminology. Although many pathologists still use the term MFH in human pathology, it should be noted that the specialists in soft tissue tumor pathology are highly skeptical about the existence of such an entity. This has been particularly well articulated and argued by Fletcher, who has dubbed the term a "meaningless diagnosis of convenience."³⁶ On

this basis there is a strong case to merge the two categories, which we have called MFH and pleomorphic sarcoma, into a group called pleomorphic-storiform sarcoma. We are in agreement with the argument of Fletcher as applied to human sarcomas. However, in our rat study we have chosen to differentiate between these two groups, as those tumors classified as pleomorphic sarcoma contained multinucleated tumor cells with marked hyperchromasia and nuclear pleomorphism, whereas those we termed MFH had, in addition to a spindle cell component, multinucleated cells with much more bland appearance (that is, with only slight hyperchromasia and nuclear pleomorphism). We therefore saw the need to separate these two groups.

The question of preneoplastic change in the capsule tissue around implanted biomaterials was only tangentially addressed in the paper by Nakamura et al.¹⁹ They described some cells showing tumorous change in one capsule around a PE implant. Our study demonstrates that the capsule tissue often presents a clearly premalignant lesion. In addition, we have been able to show that a spectrum of lesions can be distinguished from a proliferative lesion without identifiable atypical cells through preneoplastic proliferative lesions to incipient sarcoma. Nevertheless, we stress that in this attempted morphological delineation of stages in the progression toward sarcoma an element of subjectivity is present. Thus, another group of pathologists could easily have a different threshold for their diagnosis, so that what we have termed "proliferative lesion, possibly preneoplastic" could be preneoplastic, and some lesions in this latter category could be placed in the sarcoma group. Despite the arbitrary nature of the classification, a spectrum of lesions is clearly discernable in this model, which also raises the question of time course to appearance of the individual lesions. Despite the fact that the experimental design does not lend itself to providing a definitive answer, some generalizations may be attempted. As the time scale was unknown to us, we chose a study which was terminated after a time period of 8 months (short-term, for PE 3 months) and one running over 2 years, whereby because of tumor development, tissue (both tumorous and capsular) became available at various stages between 8 and 24 months. The focal proliferative lesion, that is within a restricted area at the tissue biomaterial interface a proliferate of spindle and polygonal cells, was present at 8 months in all six biomaterial groups studied at this time. Averaged across all groups, this represented 49% (56 of 114 capsules). Unfortunately, at 8 months, those lesions with proliferative foci and on the basis of some clearly atypical cells termed "possibly preneoplastic" were not homogeneously distributed among the biomaterial groups. The frequency ranged from zero in the PVC and PMMA groups to 50% (10 of 20 capsules) in the Si group. The latter, along with the PE and PU groups (22 and 33% of capsules, respectively), could be useful for molecular studies on this atypical cell population. Lesions which we could unequivocally term preneoplastic were found in none of the groups at 3 or 8 months. Deducing the time course of the various capsule lesions from the 2-year study is practically impossible. Nevertheless, some ten-

tative postulates can be made. Thus, for example, in the Si group, although from the short-term study 50% of capsules were questionably preneoplastic, the earliest sarcoma was not observed in the long-term study until week 52, compared with weeks 26 and 36 for PE and PU, respectively. On the basis of these observations it would appear that with silicone atypical cells appear at the biomaterial interface early, but the time to development of definitive sarcomas is long in relation to the other groups. Even if this statement must be made in a guarded fashion, the Si group has also the positive side of providing a 50/50 chance of a preneoplastic or possibly preneoplastic capsule under the conditions of the 2-year study design (8 of 16 capsules). From the viewpoint of statistical probability the PU group is also useful with almost 40% (8 of 21 capsules) showing either of these two lesions. Reviewing the data from the 2-year study with an eye toward the probability of obtaining a capsule lesion with at least questionable preneoplasia (from among the groups proliferative lesion, possibly preneoplastic, preneoplastic lesion, and sarcoma in the capsule) reveals the PMMA group at the top with 67% (12 of 18 capsules). This is followed by PE with 59% (19 of 32 capsules), Si with 56% (9 of 16 capsules), and PU with 52% (11 of 21 capsules). At the end of the probability list is the aluminum oxide ceramic with only 25% (4 of 16 capsules), making it a poor candidate for effective molecular studies.

The high frequency of the described lesions in the subcutaneous peri-implant capsules indicates that this animal model could be useful for tumorigenic studies on the stages of progression from proliferation through atypical proliferation to sarcoma. To our knowledge such a model has not been presented for sarcoma, in which such stages can be distinguished with a high enough incidence to make such studies feasible. An important aspect in ensuring that these preneoplastic lesions can be grasped is the use of three separate implants of similar composition in each animal. This markedly increases the probability of finding the early stages in sarcoma development by compensating for the variability of biological response from animal to animal. By using the ethically determined experimental endpoint, namely the presence of a macroscopically manifest tumor at one site, it was found that the capsules of the remaining two implant sites often revealed preneoplastic alterations.

References

1. Kim SH, Roth KA, Moser AR, Gordon JI: Transgenic mouse models that explore the multistep hypothesis of intestinal neoplasia. *J Cell Biol* 1993, 123:877-893
2. Papadimitrakopoulou VA, Shin DM, Hong WK: Molecular and cellular biomarkers for field cancerization and multistep process in head and neck tumorigenesis. *Cancer Metastasis Rev* 1996, 15:53-76
3. Baker SJ, Preisinger AC, Jessup JM, Paraskeva C, Markowitz S, Willson JK, Hamilton S, Vogelstein B: p53 gene mutations occur in combination with 17p allelic deletions as late events in colorectal tumorigenesis. *Cancer Res* 1990, 50:7717-7722
4. Cho KR, Vogelstein B: Genetic alterations in the adenoma-carcinoma sequence. *Cancer* 1992, 70(suppl 6):1727-1731
5. Powell SM, Zilz N, Beazer-Barclay Y, Bryan TM, Hamilton SR, Thibodeau SN, Vogelstein B, Kinzler KW: APC mutations occur early during colorectal tumorigenesis. *Nature* 1992, 359:235-237
6. Tanaka T, Kawamori T, Ohnishi M, Okamoto K, Mori H, Hara A: Chemoprevention of 4-nitroquinoline 1-oxide-induced oral carcinogenesis by dietary protocatechuic acid during initiation and postinitiation phases. *Cancer Res* 1994, 54:2359-2365
7. Shibata MA, Maroulakou IG, Jorcyk CL, Gold LG, Ward JM, Green JE: p53-independent apoptosis during mammary tumor progression in C3(1)/SV40 large T antigen transgenic mice: suppression of apoptosis during the transition from preneoplasia to carcinoma. *Cancer Res* 1996, 56:2998-3003
8. Pogribny IP, Miller BJ, James SJ: Alterations in hepatic p53 gene methylation patterns during tumor progression with folate/methyl deficiency in the rat. *Cancer Lett* 1997, 115:31-38
9. Wolf RF, Ng B, Weksler B, Burt M, Brennan MF: Effect of growth hormone on tumor and host in an animal model. *Ann Surg Oncol* 1994, 1:314-320
10. Madarnas P, Dube M, Rola-Pleszczynski M, Nigam VN: An animal model of Kaposi's sarcoma. II. Pathogenesis of dimethyl hydrazine induced angiosarcoma and colorectal cancer in three mouse strains. *Anticancer Res* 1992, 12:113-117
11. Dezzo B, Rady P, Morocz I, Varga E, Somba SZ, Poulsen K, Kertai P: Morphological and immunohistochemical characteristics of dimethylnitrosamine-induced malignant mesenchymal renal tumor in F-344 rats. *J Cancer Res Clin Oncol* 1990, 116:372-378
12. Clarke AR, Cummings MC, Harrison DJ: Interaction between murine germline mutations in p53 and APC predisposes to pancreatic neoplasia but not to increased intestinal malignancy. *Oncogene* 1995, 11:1913-1920
13. Brand KG, Buoен LC, Brand I: Foreign-body tumorigenesis by vinyl chloride vinyl acetate copolymer: no evidence for chemical carcinogenesis. *J Natl Cancer Inst* 1975, 54:1259-1262
14. Brand I, Buoен LC, Brand KG: Foreign-body tumors of mice: strain and sex differences in latency and incidence. *J Natl Cancer Inst* 1977, 58:1443-1447
15. Brand KG, Buoен LC, Brand I: Foreign-body tumorigenesis induced by glass, and smooth, and rough plastic: comparative study of preneoplastic events. *J Natl Cancer Inst* 1975, 55:319-322
16. Brand KG, Buoен LC, Brand I: Multiphasic incidence of foreign body-induced sarcomas. *Cancer Res* 1976, 36:3681-3683
17. Engel A, Lamm SH: Risk of sarcomas of the breast among women with breast augmentation. *Plast Reconstr Surg* 1992, 89:571-572
18. Case CP, Langkamer VG, Howell RT, Webb J, Standen G, Palmer M, Kemp A, Learmonth ID: Preliminary observations on possible pre-malignant changes in bone marrow adjacent to worn total hip arthroplasty implants. *Clin Orthop Relat Res* 1996, 329:S269-S279
19. Nakamura T, Shimizu Y, Okumura N, Matsui T, Hyon S-H, Shimamoto T: Tumorigenicity of poly-L-lactide (PLLA) plates compared with medical-grade polyethylene. *J Biomed Mater Res* 1994, 28:17-25
20. Lewis CG, Belniak RM, Plowman MC, Hopfer SM, Knight JA, Sunderman FW Jr: Intraarticular carcinogenesis bioassays of CoCrMo and TiAlV alloys in rats. *J Arthroplasty* 1995, 10:75-82
21. James SJ, Pogribna M, Miller BJ, Bolon B, Muskjelishvili L: Characterization of cellular response to silicone implants in rats: implications for foreign-body carcinogenesis. *Biomaterials* 1997, 18:667-675
22. Corallini A, Altavilla G, Pozzi L, Bignozzi F, Negrini M, Rimessi P, Gualandi F, Barbanti-Brodano G: Systemic expression of HIV-1 tat gene in transgenic mice induces endothelial proliferation and tumors of different histotypes. *Cancer Res* 1993, 53:5569-5575
23. Lindgren V, Sippola-Thiele M, Skowronski J, Wetzl E, Howley PM, Hanahan D: Specific chromosomal abnormalities characterize fibrosarcomas of bovine papillomavirus type 1 transgenic mice. *Proc Natl Acad Sci USA* 1989, 86:5025-5029
24. Rachko D, Brand KG: Chromosomal aberrations in foreign-body tumorigenesis of mice. *Proc Soc Exp Biol Med* 1983, 172:382-388
25. Brand KG, Buoен LC, Johnson KH, Brand I: Etiological factors, stages, and the role of the foreign body in foreign body tumorigenesis: a review. *Cancer Res* 1975, 35:279-286
26. Thomassen MJ, Buoен LC, Brand I, Brand KG: Foreign-body tumorigenesis in mice: DNA synthesis in surface-attached cells during preneoplasia. *J Natl Cancer Inst* 1978, 61:359-363
27. MacDonald GC, Furcht LT, Brand KG: Fibronectin in foreign body-

- induced sarcomas and preneoplastic cells. *Proc Soc Exp Biol Med* 1983, 172:89-92
28. Weinberger MA, Albert RH, Montgomery SB: Splenotoxicity associated with splenic sarcomas in rats fed high doses of D & C Red No. 9 or aniline hydrochloride. *J Natl Cancer Inst* 1985, 75:681-690
 29. Heath JC: The histogenesis of malignant tumours induced by cobalt in the rat. *Br J Cancer* 1960, 14:478-482
 30. Meachim G, Pedley RB, Williams DF: A study of sarcogenicity associated with Co-Cr-Mo particles implanted in animal muscle. *J Biomed Mater Res* 1982, 16:407-416
 31. Lewis CG, Belniak RM, Plowman MC, Hopfer SM, Knoght JA, Sunderman FW Jr: Intraarticular carcinogenesis bioassays of CoCrMo and TiAlV alloys in rats. *J Arthroplasty* 1995, 10:75-82
 32. Kass PH, Barnes WG Jr, Spangler WL, Chomel BB, Culbertson MR: Epidemiologic evidence for a causal relation between vaccination and fibrosarcoma tumorigenesis in cats. *J Am Vet Med Assoc* 1993, 203:396-405
 33. Hendrick MJ, Shofer FS, Goldschmidt MH, Haviland JC, Schelling SH, Engler SJ, Gliatto JM: Comparison of fibrosarcomas that developed at vaccination sites and at nonvaccination sites in cats: 239 cases (1991-1992). *J Am Vet Med Assoc* 1994, 205:1425-1429
 34. Hendrick MJ, Goldschmidt MH, Shofer FS, Wang YY, Somlyo AP: Postvaccinal sarcomas in the cat: epidemiology and electron probe microanalytical identification of aluminum. *Cancer Res* 1992, 52: 5391-5394
 35. Bischoff F, Bryson G: Carcinogenesis through solid state surfaces. *Prog Exp Tumor Res* 1964, 5:85-133
 36. Fletcher CD: Pleomorphic malignant fibrous histiocytoma: fact or fiction? A critical reappraisal based on 159 tumors diagnosed as pleomorphic sarcoma. *Am J Surg Pathol* 1992, 16:213-228